

Strong gravitational lensing of a 4-dimensional Einstein-Gauss-Bonnet black hole in homogeneous plasma

Xing-Hua Jin^{1,*}, Yuan-Xing Gao², and Dao-Jun Liu^{2†}

¹ *Department of Mathematics, Shanghai Business School, Shanghai 200235, China and*

² *Center for Astrophysics and Department of Physics,
Shanghai Normal University, Shanghai 200234, China*

We investigate the strong gravitational lensing of spherically symmetric black holes in the novel Einstein-Gauss-Bonnet (EGB) gravity surrounded by unmagnetised plasma medium. The deflection angle in the strong deflection limit in EGB spacetime with homogeneous plasma is derived. We find that both the coupling constant α in the novel EGB gravity and the presence of plasma can affect the radius of photon sphere, strong field limit coefficient and other lensing observables significantly. While plasma has little effect on the angular image separation and the relative magnifications as $\alpha/M^2 \rightarrow -8$ and $\alpha/M^2 \rightarrow 1$, respectively.

PACS numbers: 04.70.Dy, 95.30.Sf, 98.62.Sb, 94.20.ws

I. INTRODUCTION

Gravitational lensing is the phenomenon of deflection of light rays in a gravitational field, which has been successfully employed to explain the astronomical observations in the weak field approximation [1–4] when deflection angle is small. When the light rays approach towards the photon sphere of black hole where the gravitational field is extremely strong, the deflection angle becomes so large that the weak field method is no longer valid. It was first noticed by Darwin [5] in 1959 that the light rays passing very close to a black hole would make complete one or more loops around it before falling into the event horizon, hence an infinite series of exotic images were produced. Later, strong gravitational lensing was regained wide attention [6]. The exact lensing equation with arbitrary large value of deflection angle is obtained in 2000 [7, 8]. In 2001 Bozza et al. [9] developed a reliable and analytical method to obtain the deflection angle of Schwarzschild black hole in strong field region and they found the logarithmic divergence of the deflection angle in strong field limit. Later Bozza [10] extended the conclusion to a general asymptotically flat, static, and spherically symmetric spacetime. With the help of strong gravitational lensing it is possible to compare alternative theories of gravity [11–19] and pick up information from different compact objects [20–33]. Recently, Tsukamoto [34] proposed an improvement of the strong deflection limit analysis by the definition of a standard variable. Last year, the first image of the supermassive black hole in the Virgo Cluster galaxy M87 has been captured by the Event Horizon Telescope (EHT)[35–37], which provides us the deeper understanding of the strong gravitational physics.

One of the simplest natural extension of Einstein’s gravity by higher curvature correction is the Einstein-Gauss-

*Electronic address: jinXH@sbs.edu.cn

†Electronic address: djliu@shnu.edu.cn

Bonnet (EGB) gravity, the action of which in D -dimensional spacetime is given by

$$S = \frac{1}{16\pi} \int d^D x \sqrt{-g} \left[\frac{M_{\text{P}}^2}{2} R + \alpha \mathcal{G} \right], \quad (1)$$

where α is the coupling constant of the Gauss-Bonnet (GB) term

$$\mathcal{G} = R^{\mu\nu}{}_{\rho\sigma} R^{\rho\sigma}{}_{\mu\nu} - 4R^\mu{}_\nu R^\nu{}_\mu + R^2 = 6R^{\mu\nu}{}_{[\mu\nu} R^{\rho\sigma}{}_{\rho\sigma]}, \quad (2)$$

with $R_{\mu\nu\rho\sigma}$ the Riemann tensor, $R_{\mu\nu}$ the Ricci tensor and R the Ricci scalar. In the 4-dimensional spacetime, GB term is a total derivative [38], so it has no contribution to the gravitational dynamics. However, the role of the GB term in 4-dimensional gravity, in particular, holographic implications to the addition of it to the gravity action was studied in Ref. [39]. Notice that standard thermodynamics for AdS black holes is recovered in this way. Recently, Glavan and Lin [40] reformulate the D -dimensional EGB gravity by rescaling the coupling $\alpha \rightarrow \alpha/(D-4)$. They obtain a novel 4-dimensional EGB gravity theory in the limit $D \rightarrow 4$, where the GB term can give the nontrivial contribution of gravitational dynamics. They also have shown that it can bypass the Lovelock's theorem [41, 42] and prevent Ostrogradsky instability [43]. In addition, a novel static spherically symmetric black hole solution was obtained within this theory. Note that the black-hole solution was found earlier in the gravity theories with conformal anomaly [44] and quantum corrections [45], and recently in regularized Lovelock gravity [46], respectively.

The novel 4-dimensional EGB black holes are free from singularity problem. Their photon sphere and shadow, as well as the innermost stable circular orbit (ISCO) of a spinless test particle [47] and spinning test particle [48] around them, have been calculated. Quasinormal modes of bosonic fields [49] and fermionic fields [50] of these black hole have been investigated, and it is found that for the bosonic fields the damping rate is more sensitive than the real part of quasinormal modes by changing of the GB coupling constant α , while for the fermionic fields the damping rate usually decreases and the real part of the quasinormal modes increases with the increase of α . Konoplya and Zhidenko discussed the stability [51] of spherically symmetric black holes in the novel EGB gravity. Moreover, other topics in this new theory including the charged black holes in AdS spaces [52], the rotating black holes [53, 54], radiating black holes [55], the structure of relativistic stars [56], the thermodynamics of the black holes [57–60] and the accretion disk around the black hole [61] have also been studied.

On the other hand, it is believed that there exists plasma fluid surrounding black holes and other compact objects. When the light moves towards the compact objects through the plasma, the trajectory of light is different from the vacuum case. The theory of the light propagation in a curved spacetime in the presence of an isotropic dispersive medium was considered in the classical book of Synge [62]. Synge used the general relativistic Hamiltonian approach to deal with the geometrical optics in a dispersive medium. Furthermore, the influence of a spherically symmetric and time-independent plasma on the light deflection in Schwarzschild spacetime and Kerr spacetime was discussed in the book of Perlick [63]. The effect of plasma on the shadows of black holes and wormholes has been investigated in [64–68]. Gravitational lensing by the compact object in homogeneous and inhomogeneous plasma was considered in [69–75]. Tsupko and Bisnovatyi-Kogan [76] have obtained an analytical formula for the photon deflection angle of Schwarzschild black hole in a homogeneous plasma in the strong deflection limit.

In this work, we shall study the strong gravitational lensing by this novel 4-dimensional EGB black hole in an unmagnetized homogeneous plasma medium. The rest of the paper is organized as follows. In Sec. II, we study the photon sphere radius and the critical value of impact parameter of this novel black hole in the presence of plasma and

derive the expression for the deflection angle of light in Sec. III. In Sec. IV, we investigate the effects of plasma on the deflection angle, the coefficients and the observable quantities for gravitational lensing in the strong field limit. Finally, We end the paper with a summary in Sec. V. Throughout this paper we use the units in which $G = c = 1$.

II. PHOTON SPHERE OF AN EINSTEIN-GAUSS-BONNET BLACK HOLE IN THE PRESENCE OF PLASMA

Let us start from the line element of the EGB black hole spacetime [40], which is given by

$$ds^2 = -A(r)dt^2 + B(r)dr^2 + C(r)(d\theta^2 + \sin^2\theta d\varphi^2), \quad (3)$$

where the functions $A(r)$, $B(r)$ and $C(r)$ have respectively the following form,

$$A(r) = 1 + \frac{r^2}{2\alpha} \left(1 - \sqrt{1 + \frac{8\alpha M}{r^3}} \right), \quad (4)$$

$$B(r) = \left[1 + \frac{r^2}{2\alpha} \left(1 - \sqrt{1 + \frac{8\alpha M}{r^3}} \right) \right]^{-1}, \quad (5)$$

$$C(r) = r^2. \quad (6)$$

It has been shown that the metric is asymptotic flat by the expansion at large r . Here M is the mass of the EGB black hole and the GB coupling constant α is constrained in the range $-8 \leq \alpha/M^2 \leq 1$ [47]. For the case $0 < \alpha/M^2 \leq 1$, there are two horizons

$$r_{\pm} = M \pm \sqrt{M^2 - \alpha}. \quad (7)$$

While for the case $-8 \leq \alpha/M^2 < 0$, there is only one horizon r_+ , where the singular short radial distances $r < \sqrt[3]{-8\alpha M}$ are concealed inside this outer horizon. We will take the region $-8 \leq \alpha/M^2 \leq 1$ for the coupling constant in this paper.

We assume that the spacetime is filled with a spherically symmetric distribution of plasma with electron plasma frequency

$$\omega_p(r)^2 = \frac{4\pi e^2}{m} N(r), \quad (8)$$

where e and m are the charge of the electron and the mass of the electron respectively. The number density of the electrons $N(r)$ is the function of the radius coordinate only. The relation between the refraction index n and the photon frequency ω is given as

$$n^2 = 1 - \frac{\omega_p^2(r)}{\omega^2}. \quad (9)$$

It is found that when $\omega > \omega_p$, the photon can propagate through the plasma. On the other hand, when $\omega < \omega_p$, the photon motion is forbidden [70, 74]. Note that one has $n = 1$ in the vacuum case.

We start to calculate the strong gravitational lensing of the EGB black hole surrounded by plasma. The trajectories of photons in a curved space-time with plasma mediums, were obtained by Synge [62]. The Hamiltonian for the light rays around the black hole surrounded by plasma has the following form [77]

$$H(x, p) = \frac{1}{2} [g^{\mu\nu} p_\mu p_\nu + \omega_p^2(r)] = 0, \quad (10)$$

where p_μ is the four-momentum of the photon and $g^{\mu\nu}$ is the contravariant metric tensor. Substituing (3) into (10), we get the equation

$$0 = -\frac{p_t^2}{A(r)} + \frac{p_r^2}{B(r)} + \frac{p_\varphi^2}{C(r)} + \omega_p^2(r). \quad (11)$$

Using the Hamiltonian (10) for the photon around the EGB black hole, the paths of light rays are then described in terms of the affine parameter λ by

$$\frac{dx^\mu}{d\lambda} = \frac{\partial H}{\partial p_\mu}, \quad \frac{dp_\mu}{d\lambda} = -\frac{\partial H}{\partial x^\mu}. \quad (12)$$

Because of the spherical symmetry, we can confine the photon orbits in the equatorial plane by taking $\theta = \pi/2$ without the loss of generality. The coordinates t and φ are cyclic, leading two constants of motions which are the energy E and the angular momentum L of the photon

$$E = -p_t = \omega_\infty, \quad L = p_\varphi, \quad (13)$$

where ω_∞ is the photon frequency at infinity. From Eqs. (3) and (12), the expression for $dr/d\lambda$, $d\varphi/d\lambda$ is obtained in terms of p_r and p_φ

$$\frac{dr}{d\lambda} = \frac{\partial H}{\partial p_r} = \frac{p_r}{B(r)}, \quad (14)$$

$$\frac{d\varphi}{d\lambda} = \frac{\partial H}{\partial p_\varphi} = \frac{p_\varphi}{C(r)}. \quad (15)$$

Using Eqs. (11), (14) and (15), we obtain the equation of trajectory for a photon which is similar to the formalism in Ref. [19]

$$\left(\frac{dr}{d\varphi}\right)^2 = \frac{R_p(r)C(r)}{B(r)} \quad (16)$$

where

$$R_p = \frac{E^2}{L^2} \frac{C(r)}{A(r)} W(r) - 1, \quad (17)$$

$$W(r) = 1 - \frac{\omega_p(r)^2}{E^2} A(r). \quad (18)$$

In the case $\omega_p(r) = 0$ or equivalently, $W(r) = 1$, Eq. (16) gives the motion of light ray in vacuum.

We are interested in a photon with a given energy E that comes in from infinity, reaches a closest distance $r = r_0$, and goes out to infinity. As r_0 corresponds to the turning point of the path, $dr/d\varphi$ vanishes and $R_p(r_0) = 0$. Hereafter subscript 0 indicates the quantity at the closest distance $r = r_0$. For a light ray initially in the asymptotically flat spacetime, the impact parameter can be represented as

$$b(r_0) = \frac{L}{E} = \sqrt{\frac{C_0 W_0}{A_0}}. \quad (19)$$

With the help of Eq. (19), $R_p(r)$ can be rewritten as

$$R_p(r) = \frac{A_0 C W}{A C_0 W_0} - 1. \quad (20)$$

To find the radius of photon sphere, which is the unstable circular photon orbit of static, spherically symmetric compact objects, one can introduce a function $h(r)$ given by Perlick [75]

$$h(r)^2 = \frac{C(r)}{A(r)}W(r) = \frac{C(r)}{A(r)} \left[1 - \frac{\omega_p(r)^2}{E^2}A(r) \right]. \quad (21)$$

The photon sphere radius r_m is the biggest real root of the equation

$$\frac{d}{dr}h(r)^2 = 0. \quad (22)$$

From Eq. (22), we obtain

$$\frac{C'}{C} + \frac{W'}{W} - \frac{A'}{A} = 0, \quad (23)$$

where prime denotes the differentiation with respect to the radial coordinate r .

Now we consider the EGB black hole surrounded by homogeneous plasma, which has the following form

$$\frac{\omega_p(r)}{E} = \beta_0, \quad (24)$$

where β_0 is a positive dimensionless constant. Then we rewrite Eq. (23) as

$$r \left[\beta_0 (2\alpha^2 + r^4 + 2\alpha r^2 + 4\alpha M r) - 2\alpha^2 \right] \sqrt{\frac{8\alpha M}{r^3} + 1} = \beta_0 (16\alpha^2 M + r^5 + 2\alpha r^3 + 8\alpha M r^2) - 6\alpha^2 M. \quad (25)$$

We can solve this equation numerically to get the radius of the photon sphere which is plotted in Fig. 1. In the left panels of Fig. 1 we show the function r_m/M for $\beta_0 = 0$, $\beta_0 = 0.1$, $\beta_0 = 0.3$, $\beta_0 = 0.5$ and $\beta_0 = 0.7$ respectively, and we demonstrate that the radius of the photon sphere of the EGB black hole decreases with the increase of α/M^2 for fixed β_0 . In the right panels of Fig. 1 we show the function r_m/M for $\alpha/M^2 = -8$, $\alpha/M^2 = -4$, $\alpha/M^2 = -2$, $\alpha/M^2 = 0$, $\alpha/M^2 = 0.4$ and $\alpha/M^2 = 1$ respectively, and we find that the radius of the photon sphere of the EGB black hole increases with the increase of β_0 for fixed α/M^2 . It is clear that the presence of coupling constant α and the plasma parameter β_0 , affects the photon sphere radius significantly. In the absence of β_0 , from Eq. (25), the largest real root has a form

$$r_m = 2\sqrt{3}M \cos \left[\frac{1}{3} \cos^{-1} \left(-\frac{4\alpha}{3\sqrt{3}M^2} \right) \right], \quad (26)$$

which is the photon radius of the EGB black hole in vacuum [47]. On the other hand, in the case $\alpha = 0$, we can get the photon radius of Schwarzschild black hole with homogeneous plasma

$$r_m = \frac{3 - 4\beta_0 + \sqrt{9 - 8\beta_0}}{2(1 - \beta_0)} M, \quad (27)$$

which has been obtained in Ref. [76].

We define the critical value of the impact parameter b_c for the light ray as

$$b_c \equiv \lim_{r_0 \rightarrow r_m} \sqrt{\frac{C_0 W_0}{A_0}}. \quad (28)$$

The strong deflection limit corresponds to the limit $r_0 \rightarrow r_m$ or $b \rightarrow b_c$. From Eqs. (4), (6) and (18), the critical impact parameter is given by

$$b_c(r_m) = \sqrt{\frac{\beta_0 \left[r_m^4 \left(\sqrt{\frac{8\alpha M}{r_m^3} + 1} - 1 \right) - 2\alpha r_m^2 \right] + 2\alpha r_m^2}{2\alpha + r_m^2 \left(1 - \sqrt{\frac{8\alpha M}{r_m^3} + 1} \right)}}. \quad (29)$$

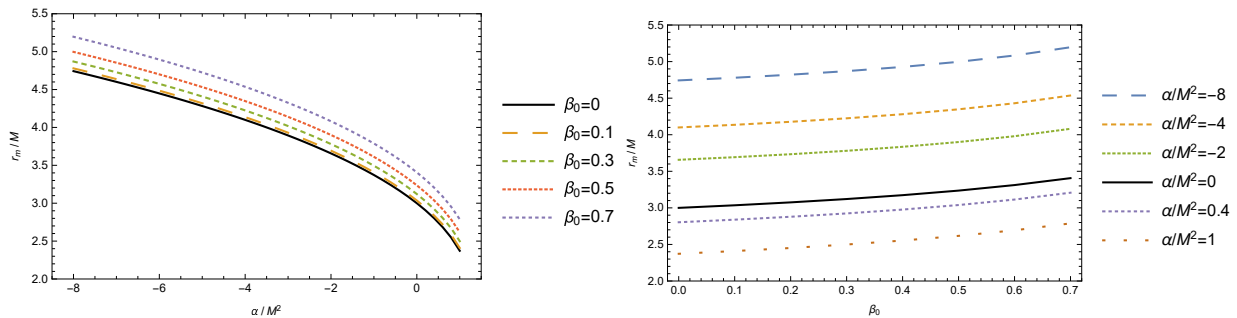


FIG. 1: Left panel: The plot of the radius of the photon sphere r_m/M as a function of α/M^2 . The five curved lines are plotted when $\beta_0 = 0$, $\beta_0 = 0.1$, $\beta_0 = 0.3$, $\beta_0 = 0.5$ and $\beta_0 = 0.7$ respectively. Right panel: The plot of the radius of the photon sphere r_m/M as a function of β_0 . The six curved lines are plotted when $\alpha/M^2 = -8$, $\alpha/M^2 = -4$, $\alpha/M^2 = -2$, $\alpha/M^2 = 0$, $\alpha/M^2 = 0.4$ and $\alpha/M^2 = 1$ respectively.

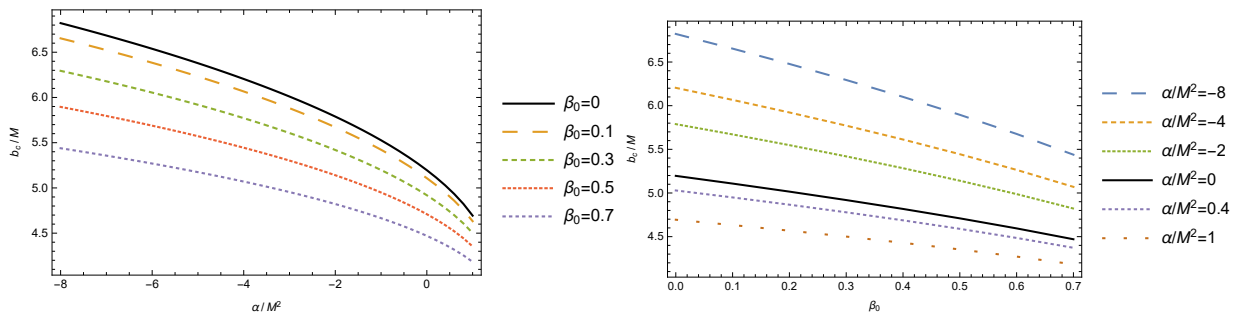


FIG. 2: Left panel: The plot of the critical impact parameter b_c/M as a function of α/M^2 . The five curved lines are plotted when $\beta_0 = 0$, $\beta_0 = 0.1$, $\beta_0 = 0.3$, $\beta_0 = 0.5$ and $\beta_0 = 0.7$ respectively. Right panel: The plot of the critical impact parameter b_c/M as a function of β_0 . The six curved lines are plotted when $\alpha/M^2 = -8$, $\alpha/M^2 = -4$, $\alpha/M^2 = -2$, $\alpha/M^2 = 0$, $\alpha/M^2 = 0.4$ and $\alpha/M^2 = 1$ respectively.

The dependence of the critical impact parameter from the coupling constant and the plasma parameters is shown in Fig. 2. The left panels of Fig. 2 presents the function b_c/M for $\beta_0 = 0$, $\beta_0 = 0.1$, $\beta_0 = 0.3$, $\beta_0 = 0.5$ and $\beta_0 = 0.7$ respectively, and it shows that the critical impact parameter of the EGB black hole decreases with the increase of α/M^2 for fixed β_0 . The right panels of Fig. 2 presents the function b_c/M for $\alpha/M^2 = -8$, $\alpha/M^2 = -4$, $\alpha/M^2 = -2$, $\alpha/M^2 = 0$, $\alpha/M^2 = 0.4$ and $\alpha/M^2 = 1$ respectively, and it shows that the critical impact parameter of the EGB black hole decreases with the increase of β_0 for fixed α/M^2 . We found that both the coupling constant and the presence of plasma have remarkable influences on the critical impact parameter.

III. STRONG GRAVITATIONAL LENSING OF EGB BLACK HOLE IN HOMOGENEOUS PLASMA

In this section, we will calculate the deflection angle of a light ray in the strong deflection limit in the EGB black hole spacetime with plasma medium. From Eq. (16), the deflection angle $\hat{\alpha}_p(r_0)$ for the photon coming from infinite to the EGB black hole in homogeneous plasma is given by

$$\hat{\alpha}_p(r_0) = I_p(r_0) - \pi, \quad (30)$$

where $I_p(r_0)$ is defined as

$$I_p(r_0) \equiv 2 \int_{r_0}^{\infty} \frac{1}{\sqrt{\frac{R_p(r)C(r)}{B(r)}}} dr. \quad (31)$$

It is found that the deflection angle increases when the closest distance r_0 decreases, and for a special point, the deflection angle will arrive at 2π which means the photon winds a complete loop around the black hole. Furthermore, when r_0 approach the radius of the photon sphere r_m the deflection angle will diverge [8]. To discuss the divergence, a new variable z is introduced [19]

$$z \equiv 1 - \frac{r_0}{r}, \quad (32)$$

Using Eqs. (4)-(6), (17) and (18), we can rewrite $I_p(r_0)$ as

$$I_p(r_0) = \int_0^1 f_p(z, r_0) dz = \int_0^1 \frac{2r_0}{\sqrt{G_p(z, r_0)}} dz, \quad (33)$$

where the function $G_p(z, r_0)$ in the EGB spacetime is given by

$$G_p(z, r_0) = \frac{R_p(z, r_0)C(z, r_0)}{B(z, r_0)}(1-z)^4 = r_0^2 \left((1-z)^2 - \frac{r_0^2 \left(\sqrt{1 - \frac{8\alpha M(z-1)^3}{r_0^3}} - 1 \right)}{2\alpha} \right) \quad (34)$$

$$\left(\frac{\left(r_0^2 \left(\sqrt{\frac{8\alpha M}{r_0^3}} + 1 - 1 \right) - 2\alpha \right) \left(-\beta_0 \left(r_0^2 \left(\sqrt{\frac{r_0^3 - 8\alpha M(z-1)^3}{r_0^3}} - 1 \right) - 2\alpha(z-1)^2 \right) - 2\alpha(z-1)^2 \right)}{\left((z-1)^2 \left(2\alpha + \beta_0 \left(r_0^2 \left(\sqrt{\frac{8\alpha M}{r_0^3}} + 1 - 1 \right) - 2\alpha \right) \right) \left(2\alpha(z-1)^2 - r_0^2 \left(\sqrt{\frac{r_0^3 - 8\alpha M(z-1)^3}{r_0^3}} - 1 \right) \right)} - 1 \right).$$

We can expand the above expression into a power series of z in the following form

$$G_p(z, r_0) = \sum_{n=1}^{\infty} c_n(r_0) z^n, \quad (35)$$

where $c_1(r_0)$ and $c_2(r_0)$ are given by

$$c_1(r_0) = \frac{\beta_0 \left(-4\alpha^2 r_0^2 \sqrt{\frac{8\alpha M}{r_0^3}} + 1 + 32\alpha^2 M r_0 + \alpha r_0^4 \left(4 - 4\sqrt{\frac{8\alpha M}{r_0^3}} + 1 \right) - 8\alpha M r_0^3 \left(\sqrt{\frac{8\alpha M}{r_0^3}} + 1 - 2 \right) \right)}{\alpha \sqrt{\frac{8\alpha M}{r_0^3}} + 1 \left(2\alpha + \beta_0 \left(r_0^2 \left(\sqrt{\frac{8\alpha M}{r_0^3}} + 1 - 1 \right) - 2\alpha \right) \right)} \quad (36)$$

$$+ \frac{\beta_0 r_0^6 \left(2 - 2\sqrt{\frac{8\alpha M}{r_0^3}} + 1 \right) + 4\alpha^2 r_0 \left(r_0 \sqrt{\frac{8\alpha M}{r_0^3}} + 1 - 3M \right)}{\alpha \sqrt{\frac{8\alpha M}{r_0^3}} + 1 \left(2\alpha + \beta_0 \left(r_0^2 \left(\sqrt{\frac{8\alpha M}{r_0^3}} + 1 - 1 \right) - 2\alpha \right) \right)},$$

and

$$\begin{aligned}
c_2(r_0) = & \frac{2\alpha^2 r_0^2 \left(96\alpha^2 M^3 r_0 + r_0^8 \left(-\sqrt{\frac{8\alpha M}{r_0^3} + 1} \right) + r_0^8 + 2\alpha r_0^6 \right)}{\alpha (8\alpha M + r_0^3)^2 \left(2\alpha + r_0^2 \left(1 - \sqrt{\frac{8\alpha M}{r_0^3} + 1} \right) \right) \left(\beta_0 \left(2\alpha + r_0^2 \left(1 - \sqrt{\frac{8\alpha M}{r_0^3} + 1} \right) \right) - 2\alpha \right)} \\
& + \frac{2\alpha^2 M^2 r_0^2 \left(128\alpha^3 + \alpha r_0^4 \left(60 - 12\sqrt{\frac{8\alpha M}{r_0^3} + 1} \right) + \alpha^2 r_0^2 \left(64 - 88\sqrt{\frac{8\alpha M}{r_0^3} + 1} \right) \right)}{\alpha (8\alpha M + r_0^3)^2 \left(2\alpha + r_0^2 \left(1 - \sqrt{\frac{8\alpha M}{r_0^3} + 1} \right) \right) \left(\beta_0 \left(2\alpha + r_0^2 \left(1 - \sqrt{\frac{8\alpha M}{r_0^3} + 1} \right) \right) - 2\alpha \right)} \\
& + \frac{2\alpha^2 M r_0^2 \left(r_0^7 \left(6 - 6\sqrt{\frac{8\alpha M}{r_0^3} + 1} \right) + \alpha r_0^5 \left(16 - 28\sqrt{\frac{8\alpha M}{r_0^3} + 1} \right) + 32\alpha^2 r_0^3 \right)}{\alpha (8\alpha M + r_0^3)^2 \left(2\alpha + r_0^2 \left(1 - \sqrt{\frac{8\alpha M}{r_0^3} + 1} \right) \right) \left(\beta_0 \left(2\alpha + r_0^2 \left(1 - \sqrt{\frac{8\alpha M}{r_0^3} + 1} \right) \right) - 2\alpha \right)} \\
& + \frac{-2\beta_0 r_0^2 (8\alpha M + r_0^3) \left(2\alpha^2 r_0^3 (\alpha - 24M^2) + 32\alpha^3 M^2 r_0 + 16\alpha^4 M + \alpha^2 r_0^5 \left(\sqrt{\frac{8\alpha M}{r_0^3} + 1} - 1 \right) \right)}{\alpha (8\alpha M + r_0^3)^2 \left(2\alpha + r_0^2 \left(1 - \sqrt{\frac{8\alpha M}{r_0^3} + 1} \right) \right) \left(\beta_0 \left(2\alpha + r_0^2 \left(1 - \sqrt{\frac{8\alpha M}{r_0^3} + 1} \right) \right) - 2\alpha \right)} \\
& + \frac{-2\beta_0 r_0^2 (8\alpha M + r_0^3) \left(6\alpha M r_0^6 \left(3\sqrt{\frac{8\alpha M}{r_0^3} + 1} - 5 \right) - 8\alpha^3 M r_0^2 \left(2\sqrt{\frac{8\alpha M}{r_0^3} + 1} + 1 \right) \right)}{\alpha (8\alpha M + r_0^3)^2 \left(2\alpha + r_0^2 \left(1 - \sqrt{\frac{8\alpha M}{r_0^3} + 1} \right) \right) \left(\beta_0 \left(2\alpha + r_0^2 \left(1 - \sqrt{\frac{8\alpha M}{r_0^3} + 1} \right) \right) - 2\alpha \right)} \\
& + \frac{-2\beta_0 r_0^2 (8\alpha M + r_0^3) \left(r_0^9 \left(3\sqrt{\frac{8\alpha M}{r_0^3} + 1} - 3 \right) + \alpha r_0^7 \left(5\sqrt{\frac{8\alpha M}{r_0^3} + 1} - 5 \right) + 4\alpha^2 M r_0^4 \left(4\sqrt{\frac{8\alpha M}{r_0^3} + 1} - 9 \right) \right)}{\alpha (8\alpha M + r_0^3)^2 \left(2\alpha + r_0^2 \left(1 - \sqrt{\frac{8\alpha M}{r_0^3} + 1} \right) \right) \left(\beta_0 \left(2\alpha + r_0^2 \left(1 - \sqrt{\frac{8\alpha M}{r_0^3} + 1} \right) \right) - 2\alpha \right)}.
\end{aligned} \tag{37}$$

It is easy to get $c_1(r_m) = 0$ in the limit $r_0 \rightarrow r_m$, while $c_2(r_m)$ is too complex in this limit. Furthermore, when $\beta_0 = 0$, i.e., in vacuum, the $c_2(r_m)$ term in the limit $r_0 \rightarrow r_m$ becomes

$$\begin{aligned}
c_2(r_m) = & \frac{96\alpha^2 M^3 r_m^3 + \alpha M^2 r_m^2 \left(128\alpha^2 - 12r_m^4 \left(\sqrt{\frac{8\alpha M}{r_m^3} + 1} - 5 \right) + 8\alpha r_m^2 \left(8 - 11\sqrt{\frac{8\alpha M}{r_m^3} + 1} \right) \right)}{\left(r_m^2 \left(\sqrt{\frac{8\alpha M}{r_m^3} + 1} - 1 \right) - 2\alpha \right) \left(r_m^3 + 8\alpha M \right)^2} \\
& + \frac{M \left(-6r_m^9 \left(\sqrt{\frac{8\alpha M}{r_m^3} + 1} - 1 \right) - 4\alpha r_m^7 \left(7\sqrt{\frac{8\alpha M}{r_m^3} + 1} - 4 \right) + 32\alpha^2 r_m^5 \right) + r_m^{10} \left(-\left(\sqrt{\frac{8\alpha M}{r_m^3} + 1} - 1 \right) \right) + 2\alpha r_m^8}{\left(r_m^2 \left(\sqrt{\frac{8\alpha M}{r_m^3} + 1} - 1 \right) - 2\alpha \right) \left(r_m^3 + 8\alpha M \right)^2}.
\end{aligned} \tag{38}$$

Since this expression is still intricate, for the sake of clarity, let's continue to look at the form under the limit $\alpha \rightarrow 0$. In the case $\beta_0 = 0$ and $\alpha = 0$, $r_m = 3M$, and Eq. (37) has a form

$$c_2(r_m) = (6M - r_m)r_m = 9M^2, \tag{39}$$

where the vacuum Schwarzschild solution is recovered. By the discussion above, we can find that the leading term of the divergence in $f_p(z, r_0)$ is z^{-1} in the strong deflection limit, which implies $I_p(r_0)$ diverges logarithmically.

One can separate $I_p(r_0)$ into two parts which are the divergent part $I_D(r_0)$ and the regular part $I_R(r_0)$

$$I_p(r_0) = I_D(r_0) + I_R(r_0). \tag{40}$$

The divergent part $I_D(r_0)$ is defined as

$$I_D(r_0) \equiv \int_0^1 f_D(z, r_0) dz, \tag{41}$$

where

$$f_D(z, r_0) \equiv \frac{2r_0}{\sqrt{c_1(r_0)z + c_2(r_0)z^2}}. \tag{42}$$

$I_D(r_0)$ can be integrated and the result is

$$I_D(r_0) = \frac{4r_0}{\sqrt{c_2(r_0)}} \log \frac{\sqrt{c_2(r_0)} + \sqrt{c_1(r_0) + c_2(r_0)}}{\sqrt{c_1(r_0)}}. \quad (43)$$

The regular part $I_R(r_0)$ is defined as

$$I_R(r_0) \equiv \int_0^1 f_R(z, r_0) dz, \quad (44)$$

where

$$f_R(z, r_0) \equiv f(z, r_0) - f_D(z, r_0). \quad (45)$$

Using a similar derivation as in Ref. [34], we obtain the deflection angle $\hat{\alpha}_p(b)$ in the strong deflection limit $r_0 \rightarrow r_m$ or $b \rightarrow b_c$ in the EGB black hole with homogeneous plasma

$$\hat{\alpha}_p(b) = -\bar{a} \log \left(\frac{b}{b_c} - 1 \right) + \bar{b} + O((b - b_c) \log(b - b_c)). \quad (46)$$

The coefficients \bar{a} and \bar{b} are obtained as

$$\bar{a} = \sqrt{\frac{2B_m}{C_m \left[\frac{(CW)_m''}{(CW)_m} - \frac{A_m''}{A_m} \right]}}, \quad (47)$$

$$\bar{b} = \bar{a} \log \left\{ r_m^2 \left[\frac{(CW)_m''}{(CW)_m} - \frac{A_m''}{A_m} \right] \right\} + I_{Rp}(r_m) - \pi, \quad (48)$$

where the subscript m denotes the quantities at $r = r_m$. In the vacuum case, i.e., $\beta_0 = 0$, and the coupling constant $\alpha = 0$, \bar{a} and \bar{b} will reduce to the formalism in Ref. [34], which are the coefficients of a Schwarzschild black hole without plasma.

The numerical results of the strong field limit coefficients \bar{a} and \bar{b} are shown in Fig. 3 and Fig. 4. The left panels of Fig. 3 show the strong field limit coefficient \bar{a} for $\beta_0 = 0$, $\beta_0 = 0.1$, $\beta_0 = 0.3$, $\beta_0 = 0.5$ and $\beta_0 = 0.7$ respectively. We find that the strong field limit coefficient \bar{a} increases with the increase of the coupling constant α/M^2 for fixed β_0 . From the right panels of Fig. 3, which refers to the strong field limit coefficient \bar{a} for $\alpha/M^2 = -8$, $\alpha/M^2 = -4$, $\alpha/M^2 = -2$, $\alpha/M^2 = 0$, $\alpha/M^2 = 0.4$ and $\alpha/M^2 = 1$ respectively, we find that the strong field limit coefficient \bar{a} increases with the increase of the plasma parameter β_0 for fixed α/M^2 . In the left panels of Fig. 4, we illustrate the strong field limit coefficient \bar{b} for $\beta_0 = 0$, $\beta_0 = 0.1$, $\beta_0 = 0.3$, $\beta_0 = 0.5$ and $\beta_0 = 0.7$ respectively, and show that the strong field limit coefficient \bar{b} decreases with the increase of the coupling parameter α/M^2 for fixed β_0 . From the right panels of Fig. 4, which refers to the strong field limit coefficient \bar{b} for $\alpha/M^2 = -8$, $\alpha/M^2 = -4$, $\alpha/M^2 = -2$, $\alpha/M^2 = 0$, $\alpha/M^2 = 0.4$ and $\alpha/M^2 = 1$ respectively, we find that the strong field limit coefficient \bar{b} increases with the increase of the plasma parameter β_0 for fixed α/M^2 . Obviously, the strong field limit coefficients \bar{a} and \bar{b} are influenced by the choice of coupling constant α and plasma parameter β_0 .

IV. OBSERVABLES IN THE STRONG DEFLECTION LIMIT

In this section we consider the observables of the strong gravitational lensing by the EGB black hole in the presence of a uniform plasma. We are interested in the case where the observer, the lens and the source are nearly in alignment,

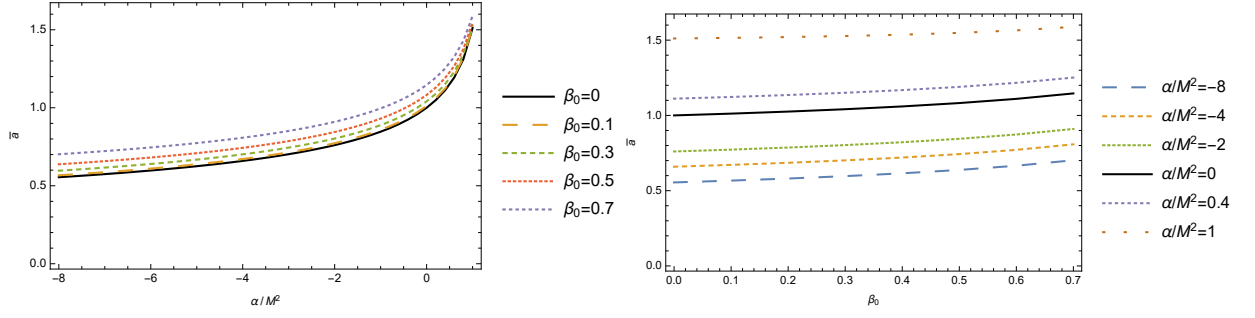


FIG. 3: Left panel: The plot of the strong field limit coefficients \bar{a} as a function of α/M^2 . The five curved lines are plotted when $\beta_0 = 0$, $\beta_0 = 0.1$, $\beta_0 = 0.3$, $\beta_0 = 0.5$ and $\beta_0 = 0.7$ respectively. Right panel: The plot of the strong field limit coefficients \bar{a} as a function of β_0 . The six curved lines are plotted when $\alpha/M^2 = -8$, $\alpha/M^2 = -4$, $\alpha/M^2 = -2$, $\alpha/M^2 = 0$, $\alpha/M^2 = 0.4$ and $\alpha/M^2 = 1$ respectively.

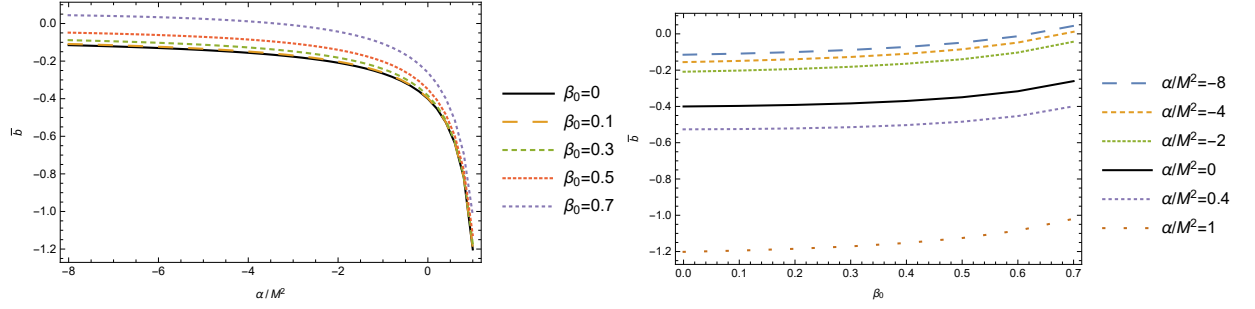


FIG. 4: Left panel: The plot of the strong field limit coefficients \bar{b} as a function of α/M^2 . The five curved lines are plotted when $\beta_0 = 0$, $\beta_0 = 0.1$, $\beta_0 = 0.3$, $\beta_0 = 0.5$ and $\beta_0 = 0.7$ respectively. Right panel: The plot of the strong field limit coefficients \bar{b} as a function of β_0 . The six curved lines are plotted when $\alpha/M^2 = -8$, $\alpha/M^2 = -4$, $\alpha/M^2 = -2$, $\alpha/M^2 = 0$, $\alpha/M^2 = 0.4$ and $\alpha/M^2 = 1$ respectively.

and the source and the observer are very far from the lens. The distance between the lens and the source, and the distance between the lens and the observer are represented by D_{LS} and D_{OL} respectively. D_{OS} is the distance between the observer and the source, and $D_{OS} = D_{LS} + D_{OL}$. β denotes the angular position with respect to the optical axis of the source. θ is the angular position with respect to the optical axis of the image and can be expressed as $\theta = b/D_{OL}$. Thus the lens equation can be written as [10]

$$\beta = \theta - \frac{D_{LS}}{D_{OS}} \Delta\alpha_n, \quad (49)$$

where $\Delta\alpha_n = \alpha - 2n\pi$ is the offset of deflection angle, and n denotes the loop numbers of the light ray around the light sphere.

The angular position θ_n between the lens and the n -th relativistic image and the magnification of the n -th relativistic image μ_n can be obtained approximately as

$$\theta_n = \theta_n^0 + \frac{b_c(\beta - \theta_n^0)D_{OS}}{\bar{a}D_{LS}D_{OL}} \exp\left(\frac{\bar{b} - 2n\pi}{\bar{a}}\right), \quad (50)$$

$$\mu_n = \frac{b_c^2 D_{OS}}{\bar{a}\beta D_{OL}^2 D_{LS}} \exp\left(\frac{\bar{b} - 2n\pi}{\bar{a}}\right) \left[1 + \exp\left(\frac{\bar{b} - 2n\pi}{\bar{a}}\right)\right]. \quad (51)$$

Here θ_n^0 is the angular position corresponding to the case that the light ray winds completely $2n\pi$ and can be expressed as

$$\theta_n^0 = \frac{b_c}{D_{OL}} \left[1 + \exp\left(\frac{\bar{b} - 2n\pi}{\bar{a}}\right) \right]. \quad (52)$$

In the limit $n \rightarrow \infty$, we can find the relation between the critical impact parameter b_c and the asymptotic position θ_∞ approached by a set of images

$$\theta_\infty = \frac{b_c}{D_{OL}}. \quad (53)$$

Since the outermost relativistic image is the brightest, one can use the observable s to describe the separation between this first image θ_1 and all the others packed images at θ_∞ [10]. The other observable \mathcal{R} represents the ratio of the received flux between this first image and all the others images [10]. Using Eqs. (50) and (51), the angular separation s and the ratio of the flux \mathcal{R} can be obtained as

$$s = \theta_1 - \theta_\infty = \theta_\infty \exp\left(\frac{\bar{b} - 2\pi}{\bar{a}}\right), \quad (54)$$

$$\mathcal{R} = \frac{\mu_1}{\sum_{n=2}^{\infty} \mu_n} = \exp\left(\frac{2\pi}{\bar{a}}\right). \quad (55)$$

If the observables s , θ_∞ and \mathcal{R} are available, the coefficients \bar{a} and \bar{b} in the strong deflection limit and the critical impact parameter b_c can be obtained easily by

$$\bar{a} = \frac{2\pi}{\log \mathcal{R}}, \quad (56)$$

$$\bar{b} = \bar{a} \log\left(\frac{\mathcal{R}s}{\theta_\infty}\right), \quad (57)$$

$$b_c = \theta_\infty D_{OL}. \quad (58)$$

Then one can numerically compute the above value by measuring the observables s , θ_∞ and \mathcal{R} and study their difference with the corresponding theoretical coefficients.

From recently observation [35], the distance between the supermassive black hole M87* and us is $D_{OL} = 16.8 \pm 0.8$ Mpc, and its mass is $M = 4.28 \times 10^9 M_\odot$ where M_\odot is the mass of the sun. The lens is supposed to be the black hole M87* described by the EGB black hole. With these data we can estimate the values of the angular image position θ_∞ , the angular image separation s and the relative magnifications r of the relativistic images which is defined as $r = 2.5 \log_{10} \mathcal{R}$. Figs. 5-7 show the behaviors of these observables and the influences on them by the choince of coupling constant α and plasma parameter β_0 .

The left panels of Fig. 5 show the value of θ_∞ as function of α/M^2 for $\beta_0 = 0$, $\beta_0 = 0.1$, $\beta_0 = 0.3$, $\beta_0 = 0.5$ and $\beta_0 = 0.7$ respectively. As the coupling constant α/M^2 increases, the angular image position decreases for fixed β_0 . The right panels of Fig. 5 show the value of θ_∞ as function of β_0 for $\alpha/M^2 = -2$, $\alpha/M^2 = 0$, $\alpha/M^2 = 0.4$ and $\alpha/M^2 = 1$ respectively. As the plasma parameter β_0 increases, the angular image position decreases for fixed α/M^2 .

As shown in the left panels of Fig. 6, the value of s is expressed as a function of α/M^2 for $\beta_0 = 0$, $\beta_0 = 0.1$, $\beta_0 = 0.3$, $\beta_0 = 0.5$ and $\beta_0 = 0.7$ respectively. As the coupling constant α/M^2 increases, the angular image separation increases for fixed β_0 . It is shown that in the right panels of Fig. 6, the value of s is expressed as function of β_0 for $\alpha/M^2 = -2$, $\alpha/M^2 = 0$, $\alpha/M^2 = 0.4$ and $\alpha/M^2 = 1$ respectively. As the plasma parameter β_0 increases, the

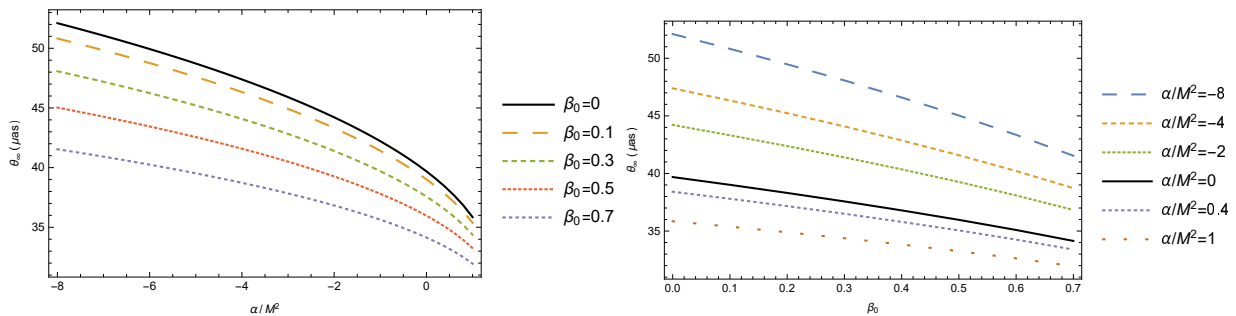


FIG. 5: Left panel: The plot of the angular image position θ_∞ as a function of α/M^2 . The five curved lines are plotted when $\beta_0 = 0$, $\beta_0 = 0.1$, $\beta_0 = 0.3$, $\beta_0 = 0.5$ and $\beta_0 = 0.7$ respectively. Right panel: The plot of the angular image position θ_∞ as a function of β_0 . The six curved lines are plotted when $\alpha/M^2 = -8$, $\alpha/M^2 = -4$, $\alpha/M^2 = -2$, $\alpha/M^2 = 0$, $\alpha/M^2 = 0.4$ and $\alpha/M^2 = 1$ respectively.

angular image separation increases for fixed α/M^2 . Interestingly, as $\alpha/M^2 \rightarrow -8$ for different plasma parameter β_0 , the angular image separation converges to the value at $\alpha/M^2 = -8$ in the vacuum case, which means plasma has little effect on the angular image separation.

In the left panels of Fig. 7, we show the value of relative magnifications as function of α/M^2 for $\beta_0 = 0$, $\beta_0 = 0.1$, $\beta_0 = 0.3$, $\beta_0 = 0.5$ and $\beta_0 = 0.7$ respectively. As the coupling constant α/M^2 increases, the relative magnifications decreases for fixed β_0 . In the right panels of Fig. 7, we show the value of relative magnifications as function of β_0 for $\alpha/M^2 = -2$, $\alpha/M^2 = 0$, $\alpha/M^2 = 0.4$ and $\alpha/M^2 = 1$ respectively. As the plasma parameter β_0 increases, the relative magnifications decreases for fixed α/M^2 . We find that as $\alpha/M^2 \rightarrow 1$ for different plasma parameter β_0 , the relative magnifications converges to the value at $\alpha/M^2 = 1$ in the vacuum case, which means plasma has little influence on the relative magnifications.

In Table I, we list the numerical estimates of the observables as well as strong field limit coefficients of a EGB black hole in uniform plasma. The parameter $\beta_0 = 0$ corresponds to the case of the EGB black hole in vacuum and $\alpha = 0$ means the case of Schwarzschild black hole in homogeneous plasma. From Table I, we can easily obtain the differences between the Schwarzschild black hole and the EGB black hole, as well as the EGB black hole with various plasma parameter.

V. CONCLUSIONS

In this work, we have investigated the strong gravitational lensing generated by a 4-dimensional Einstein-Gauss-Bonnet black hole in a plasma. In the presence of plasma around the black hole, the trajectory of a photon differs from the null geodesic in vacuum, resulting in the changes of the deflection angle of light. Using Hamilton's equation of the light ray in plasma with a frequency dependent refraction index, we have derived the equation of motion for light rays in the novel 4-dimensional EGB black hole. Furthermore, we numerically obtained the theoretical strong field limit parameters for the lensing by the black hole in a uniform plasma. Among these parameters we found that the radius of the photon sphere r_m , the critical impact parameter b_c and the strong field limit coefficient \bar{b} decrease monotonically, while the strong field limit coefficient \bar{a} increases, with the increase of the coupling constant α/M^2 for fixed value of

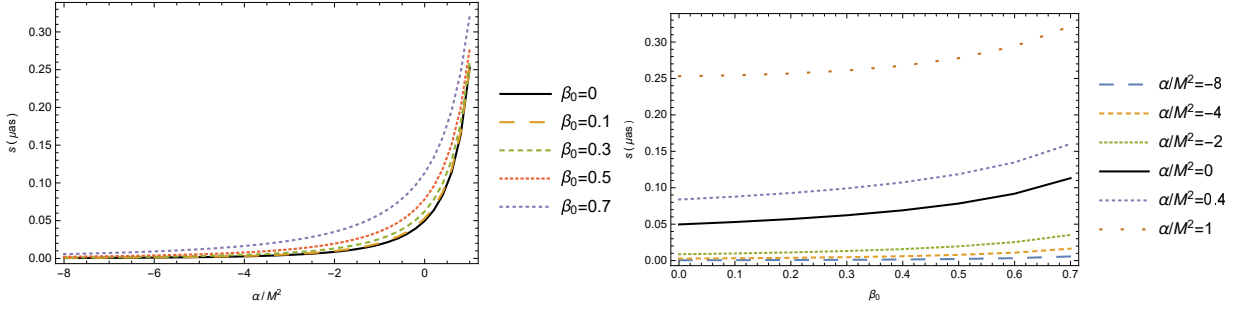


FIG. 6: Left panel: The plot of the angular image separation s as a function of α/M^2 . The five curved lines are plotted when $\beta_0 = 0$, $\beta_0 = 0.1$, $\beta_0 = 0.3$, $\beta_0 = 0.5$ and $\beta_0 = 0.7$ respectively. Right panel: The plot of the angular image separation s as a function of β_0 . The six curved lines are plotted when $\alpha/M^2 = -8$, $\alpha/M^2 = -4$, $\alpha/M^2 = -2$, $\alpha/M^2 = 0$, $\alpha/M^2 = 0.4$ and $\alpha/M^2 = 1$ respectively.

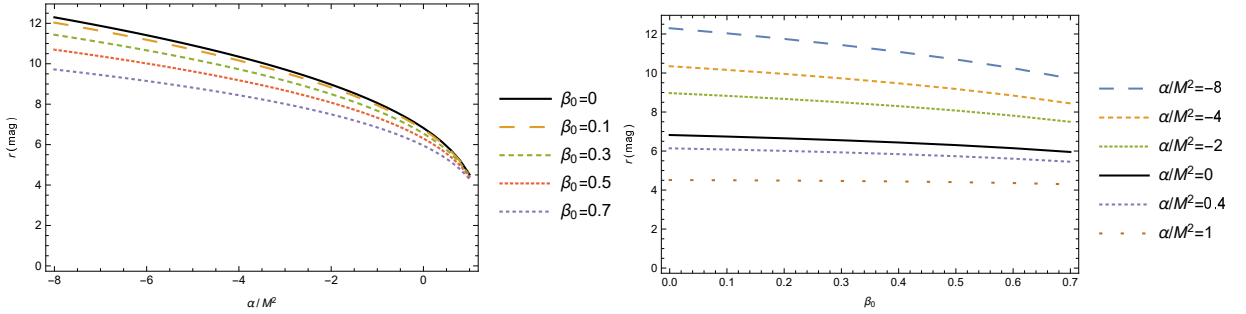


FIG. 7: Left panel: The plot of the relative magnifications r as a function of α/M^2 . The five curved lines are plotted when $\beta_0 = 0$, $\beta_0 = 0.1$, $\beta_0 = 0.3$, $\beta_0 = 0.5$ and $\beta_0 = 0.7$ respectively. Right panel: The plot of the relative magnifications r as a function of β_0 . The six curved lines are plotted when $\alpha/M^2 = -8$, $\alpha/M^2 = -4$, $\alpha/M^2 = -2$, $\alpha/M^2 = 0$, $\alpha/M^2 = 0.4$ and $\alpha/M^2 = 1$ respectively.

plasma parameter β_0 . On the other hand, for a fixed value of the coupling constant α/M^2 , with the increase of the plasma parameter β_0 , r_m , \bar{a} and \bar{b} increase, but b_c decreases monotonically. Modelling the supermassive M87* with this EGB black hole, we have estimated the observables including the angular image position θ_∞ , the angular image separation s and the relative magnifications r of the relativistic images in the uniform plasma. We have shown that among these observables, when the coupling parameter α/M^2 increases for fixed plasma parameter β_0 , the angular image position θ_∞ and the relative magnifications r decrease, while the angular image separation s increases. When the plasma parameter β_0 increases for fixed coupling constant α/M^2 , the angular image position θ_∞ and the relative magnifications r decrease, but the angular image separation s increases. Above all, both the coupling constant α and plasma parameter β_0 have significant effects on the parameters and observables in strong gravitational lensing. Interestingly, it is found that plasma has little effect on the angular image separation as $\alpha/M^2 \rightarrow -8$ and the relative magnifications as $\alpha/M^2 \rightarrow 1$, respectively.

Theoretically we can use the observations on strong gravitational lensing to test this modified gravity. But the relativistic images of strong gravitational lensing are so faint that it is hard to detect. However, with the improvement of technology, we wish observations in the future may provide the opportunity to distinguish the EGB black hole from

β_0	α/M^2	$\theta_\infty(\mu\text{as})$	$s(\mu\text{as})$	$r(\text{mag})$	b_c/R_s	\bar{a}	\bar{b}
	-8	52.10	0.000511	12.30	3.41	0.555	-0.1151
	-4	47.39	0.00272	10.35	3.10	0.659	-0.1558
	-2	44.21	0.00867	8.97	2.89	0.760	-0.2087
0	0	39.69	0.0497	6.82	2.60	1	-0.4003
	0.4	38.41	0.0838	6.14	2.51	1.111	-0.5264
	1	35.85	0.253	4.51	2.35	1.511	-1.2017
	-8	50.82	0.000644	12.03	3.33	0.567	-0.1088
	-4	46.33	0.00320	10.16	3.03	0.671	-0.1490
	-2	43.31	0.00980	8.83	2.83	0.773	-0.2024
0.1	0	39.01	0.0530	6.74	2.55	1.012	-0.3971
	0.4	37.80	0.0878	6.08	2.47	1.123	-0.5249
	1	35.38	0.254	4.50	2.32	1.515	-1.1947
	-8	48.08	0.000111	11.43	3.15	0.597	-0.08858
	-4	44.08	0.00473	9.73	2.89	0.701	-0.1274
	-2	41.39	0.00132	8.50	2.71	0.803	-0.1815
0.3	0	37.57	0.0622	6.55	2.46	1.041	-0.3833
	0.4	36.50	0.0991	5.93	2.39	1.150	-0.5144
	1	34.38	0.261	4.47	2.25	1.527	-1.1715
	-8	45.03	0.00220	10.70	2.95	0.638	-0.04854
	-4	41.58	0.00788	9.18	2.72	0.743	-0.08515
	-2	39.26	0.00196	8.08	2.57	0.845	-0.1400
0.5	0	35.97	0.0783	6.30	2.35	1.082	-0.3494
	0.4	35.05	0.119	5.73	2.29	1.190	-0.4843
	1	33.25	0.278	4.41	2.18	1.548	-1.1255
	-8	41.54	0.00574	9.72	2.72	0.702	0.04408
	-4	38.73	0.0165	8.44	2.54	0.808	0.01158
	-2	36.83	0.0352	7.50	2.41	0.910	-0.04313
0.7	0	34.14	0.113	5.95	2.24	1.146	-0.2606
	0.4	33.40	0.160	5.45	2.19	1.251	-0.3993
	1	31.95	0.322	4.30	2.09	1.588	-1.0194

TABLE I: Numerical estimation for the observables and the strong deflection limit coefficients for EGB black holes supposed to describe the object at the center of our Galaxy. $R_s = 2GM/c^2$ is the Schwarzschild radius.

those in general relativity.

Acknowledgments

This work is supported in part by Science and Technology Commission of Shanghai Municipality under Grant No. 12ZR1421700 and Shanghai Normal University KF201813.

Note added in proof: After this work was completed, we learned a similar work by Islam et al. [78], which appeared in arXiv a couple of days before.

-
- [1] P. Schneider, J. Ehlers, and E. E. Falco, *Gravitational Lenses* (Springer-Verlag, Berlin, 1992).
 - [2] A. O. Petters, H. Levine, and J. Wambsganss, *Singularity Theory and Gravitational Lensing* (Birkhauser, Boston, 2001).
 - [3] P. Schneider, C. S. Kochanek, and J. Wambsganss, *Gravitational Lensing: Strong, Weak and Micro, Lecture Notes of the 33rd Saas-Fee Advanced Course*, edited by G. Meylan, P. Jetzer, and P. North (Springer-Verlag, Berlin, 2006).
 - [4] M. Bartelmann, *Class. Quant. Grav.* **27**, 233001 (2010).
 - [5] C. Darwin, *Proc. of the Royal Soc. of London* **249**, 180 (1959).
 - [6] R. D. Atkinson, *Astron. J.* **70**, 517 (1965); J. P. Luminet, *Astron. Astrophys.* **75**, 228 (1979); H. C. Ohanian, *Am. J. Phys.* **55**, 428 (1987); R. J. Nemiroff, *Am. J. Phys.* **61**, 619 (1993).
 - [7] S. Frittelly, T. P. Kling and E. T. Newman, *Phys. Rev. D* **61**, 064021 (2000).
 - [8] K. S. Virbhadra and G. F. R. Ellis, *Phys. Rev. D* **62** 084003 (2000).
 - [9] V. Bozza, S. Capozziello, G. Iovane and G. Scarpetta, *Gen. Rel. Grav.* **33**, 1535 (2001).
 - [10] V. Bozza, *Phys. Rev. D* **66**, 103001 (2002).
 - [11] C. M. Claudel, K. S. Virbhadra and G. F. R. Ellis, *J. Math. Phys.* **42**, 818 (2001).
 - [12] W. Hasse and V. Perlick, *Gen. Relativ. Gravit.* **34**, 415 (2002).
 - [13] S. V. Iyer and A. O. Petters, *Gen. Rel. Grav.* **39**, 1563 (2007).
 - [14] K. S. Virbhadra, C. R. Keeton, *Phys. Rev. D* **77**, 124014 (2008).
 - [15] V. Bozza, *Phys. Rev. D* **78**, 103005 (2008).
 - [16] V. Bozza, *Gen. Rel. Grav.* **42**, 2269 (2010).
 - [17] T. Ghosh and S. Sengupta, *Phys. Rev. D* **81**, 044013 (2010).
 - [18] S. Wei, Y. Liu, C. Fu and K. Yang, *JCAP* **1210**, 053 (2012);
 - [19] N. Tsukamoto, *Phys. Rev. D* **94**, 124001 (2016).
 - [20] V. Bozza, *Phys. Rev. D* **67**, 103006 (2003).
 - [21] S.E. Vázquez, E.P. Esteban, *Nuovo Cimento B Ser.* **119**, 489 (2004).
 - [22] V. Bozza, F. de Luca, G. Scarpetta, M. Sereno, *Phys. Rev. D* **72**, 083003 (2005).
 - [23] V. Bozza, F. de Luca, G. Scarpetta, *Phys. Rev. D* **74**, 063001 (2006).
 - [24] S. Chen, J. Jing, *Class. Quantum Gravity* **27**, 225006 (2010).
 - [25] S. Chen, Y. Liu, J. Jing, *Phys. Rev. D* **83**, 124019 (2011).
 - [26] P.V.P. Cunha, C.A.R. Herdeiro, E. Radu, H.F. Rúnarsson, *Phys. Rev. Lett.* **115**, 211102 (2015).
 - [27] R.T. Cavalcanti, A. Goncalves da Silva, R. da Rocha, *Class. Quantum Gravity* **33**, 215007 (2016).
 - [28] G.N. Gyulchev, S.S. Yazadjiev, *Phys. Rev. D* **78**, 083004 (2008).
 - [29] S. Sahu, M. Patil, D. Narasimha, P.S. Joshi, *Phys. Rev. D* **86**, 063010 (2012).
 - [30] S. Sahu, M. Patil, D. Narasimha, P.S. Joshi, *Phys. Rev. D* **88**, 103002 (2013).
 - [31] P.K.F. Kuhfittig, *Eur. Phys. J. C* **74**, 2818 (2014).
 - [32] K.K. Nandi, Y.Z. Zhang, A.V. Zakharov, *Phys. Rev. D* **74**, 024020 (2006).
 - [33] N. Tsukamoto, T. Harada, K. Yajima, *Phys. Rev. D* **86**, 104062 (2012).
 - [34] N. Tsukamoto, *Phys. Rev. D* **95**, 064035 (2017)
 - [35] The Event Horizon Telescope Collaboration, *Astrophys. J. Lett.* **875**, L1 (2019).
 - [36] The Event Horizon Telescope Collaboration, *Astrophys. J. Lett.* **875**, L5 (2019).

- [37] The Event Horizon Telescope Collaboration, *Astrophys. J. Lett.* **875**, L6 (2019).
- [38] C. Lanczos, *Annals Math.* **39**, 842 (1938).
- [39] O. Miskovic and R. Olea, *Phys. Rev. D* **79**, 124020 (2009) [arXiv:0902.2082 [hep-th]].
- [40] D. Glavan and C. Lin, *Phys. Rev. Lett.* **124**, no. 8, 081301 (2020) [arXiv:1905.03601 [gr-qc]].
- [41] D. Lovelock, *J. Math. Phys.* **12**, 498 (1971).
- [42] D. Lovelock, *J. Math. Phys.* **13**, 874 (1972).
- [43] R. P. Woodard, *Scholarpedia* **10**, no. 8, 32243 (2015) [arXiv:1506.02210 [hep-th]].
- [44] R. G. Cai, L. M. Cao and N. Ohta, *JHEP* **1004**, 082 (2010) [arXiv:0911.4379 [hep-th]].
- [45] G. Cognola, R. Myrzakulov, L. Sebastiani and S. Zerbini, *Phys. Rev. D* **88**, no. 2, 024006 (2013) [arXiv:1304.1878 [gr-qc]].
- [46] A. Casalino, A. Colleaux, M. Rinaldi and S. Vicentini, arXiv:2003.07068 [gr-qc].
- [47] M. Guo and P. C. Li, arXiv:2003.02523 [gr-qc].
- [48] Y. P. Zhang, S. W. Wei and Y. X. Liu, arXiv:2003.10960 [gr-qc].
- [49] R. A. Konoplya and A. F. Zinhailo, arXiv:2003.01188 [gr-qc].
- [50] M. S. Churilova, arXiv:2004.00513 [gr-qc].
- [51] R. A. Konoplya and A. Zhidenko, arXiv:2003.12492 [gr-qc].
- [52] P. G. S. Fernandes, arXiv:2003.05491 [gr-qc].
- [53] S. W. Wei and Y. X. Liu, arXiv:2003.07769 [gr-qc].
- [54] R. Kumar and S. G. Ghosh, arXiv:2003.08927 [gr-qc].
- [55] S. G. Ghosh and S. D. Maharaj, arXiv:2003.09841 [gr-qc].
- [56] D. D. Doneva and S. S. Yazadjiev, arXiv:2003.10284 [gr-qc].
- [57] K. Hegde, A. Naveena Kumara, C. L. A. Rizwan, A. K. M. and M. S. Ali, arXiv:2003.08778 [gr-qc].
- [58] D. V. Singh and S. Siwach, arXiv:2003.11754 [gr-qc].
- [59] C. Y. Zhang, P. C. Li and M. Guo, arXiv:2003.13068 [hep-th].
- [60] S. A. Hosseini Mansoori, arXiv:2003.13382 [gr-qc].
- [61] C. Liu, T. Zhu and Q. Wu, arXiv:2004.01662 [gr-qc].
- [62] J. L. Synge, *Relativity: the General Theory* (North-Holland Publishing Company, Amsterdam, 1960).
- [63] V. Perlick, *Ray Optics, Fermat's Principle, and Applications to General Relativity* (Springer-Verlag, Berlin, 2000).
- [64] G. Bisnovaty-Kogan and O. Tsupko, *Universe* **3**, 57 (2017).
- [65] A. Abdujabbarov, B. Toshmatov, Z. Stuchlk, and B. Ahmedov, *Int. J. Mod. Phys. D* **26**, 1750051 (2016).
- [66] V. Perlick and O. Yu. Tsupko, *Phys. Rev. D* **95**, 104003, (2017).
- [67] A. Abdujabbarov, B. Juraev, B. Ahmedov, and Z. Stuchlk, *Astrophys. Space Sci.* **361**, 226 (2016).
- [68] Y. Huang, Y. P. Dong and D. J. Liu, *Int. J. Mod. Phys. D* **27**, no.12, 1850114 (2018)
- [69] G. S. Bisnovaty-Kogan and O. Yu. Tsupko, *Gravitation and Cosmology* **15**, 20 (2009).
- [70] G. S. Bisnovaty-Kogan and O. Yu. Tsupko, *Mon. Not. Roy. Astr. Soc.* **404**, 1790 (2010).
- [71] V. Morozova, B. Ahmedov, and A. Tursunov, *Astrophys. Space Sci.* **346**, 513 (2013)
- [72] X. Er and S. Mao, *Mon. Not. Roy. Astron. Soc.* **437**, 2180 (2013)
- [73] A. Farruh, A. Bobomurat and A. Ahmadjon; *Phys. Rev. D* **92**, 084005 (2015).
- [74] A. Rogers, *Mon. Not. Roy. Astron. Soc.* **451**, 4536 (2015)
- [75] V. Perlick, O. Yu. Tsupko and G. S. Bisnovaty-Kogan, *Phys. Rev. D* **92**, 104031 (2015))
- [76] O. Yu. Tsupko and G. S. Bisnovaty-Kogan, *Phys. Rev. D* **87**, 124009 (2013).
- [77] R. Kulsrud and A. Loeb, *Phys. Rev. D* **45**, 525 (1992).
- [78] S. U. Islam, R. Kumar and S. G. Ghosh, arXiv:2004.01038 [gr-qc].